Received: 6 June 2024 | Accepted: 26 August 2024

DOI: 10.1002/jcp.31428

RESEARCH ARTICLE

Journal of Cellular Physiology WILEY

Mineralocorticoid receptor activates postnatal adiposity in zebrafish lacking proopiomelanocortin

Jithine J. Rajeswari | Erin Faught | Helio Santos | Mathilakath M. Vijayan

Department of Biological Sciences, University of Calgary, Calgary, Alberta, Canada

Correspondence
Mathilakath M. Vijayan, Department of Biological Sciences, University of Calgary, Calgary, AB, T2N1N4 Canada.
Email: matt.vijayan@ucalgary.ca

Present addresses
Erin Faught, Institute of Biology, Leiden University, Leiden, The Netherlands.

Helio Santos, Laboratório de Processamento de Tecidos, Universidade Federal de São João Del Rei, Avenida Sebastião Gonçalves Coelho, Divinópolis, Brazil.

Funding information
Natural Sciences and Engineering Research Council of Canada

Abstract

The proopiomelanocortin (Pomc)-derived peptides, including adrenocorticotropic hormone and α-melanocyte stimulating hormone (α-Msh), play both a central and a peripheral role in modulating the stress response. The central role is predominantly associated with nutrient homeostasis, while peripherally they play an important role in the synthesis of glucocorticoids (GCs) in response to stress. Pomc mutations are a major risk factor in the development of early-onset childhood obesity in humans. This is attributed primarily to their central effects on melanocortin receptor dysfunction leading to hyperphagia and reduced energy expenditure, while the peripheral mechanism contributing to obesity has largely been unexplored. Here, we tested the hypothesis that Pomc mutation-mediated adrenal insufficiency and the associated changes in GC signaling contribute to postnatal adiposity using zebrafish as a model. We generated a ubiquitous Pomc knockout zebrafish that mimicked the mammalian mutant phenotype of adrenal insufficiency and enhanced adiposity. The loss of Pomc inhibited stress-induced cortisol production and reprogrammed GC signaling by reducing glucocorticoid receptor responsiveness, whereas the mineralocorticoid receptor (Mr) signaling was enhanced. Larval feeding led to enhanced growth and adipogenesis in the Pomc mutants, and this was inhibited by eplerenone, an Mr antagonist. Altogether, our results underscore a key role for Mr signaling in early developmental adipogenesis and a possible target for therapeutic intervention for early-onset childhood obesity due to Pomc dysfunction.

KEYWORDS
corticosteroid receptors, cortisol, obesity, pomca, stress, zebrafish

1 | INTRODUCTION

The activation of the hypothalamus-pituitary-adrenal (HPA) axis is a highly conserved response to stress in vertebrates leading to the production of glucocorticoids (GCs) (Charmandari et al., 2005; Nicolaides et al., 2015). The two key neuropeptides, the corticotropin-releasing hormone (Crh) from the hypothalamus and the adrenocorticotropic hormone (Acth) from the pituitary, orchestrate the stress-induced GC biosynthesis in the adrenal cortex (Charmandari et al., 2005; Nicolaides et al., 2015). The Acth is produced in the anterior pituitary from a pro-hormone, the proopiomelanocortin (Pomc), which is enzymatically cleaved by the pro-hormone convertases (Harno et al., 2018). Acth binds to Mc2r, a G-protein coupled receptor, in the adrenal cortex to stimulate GC synthesis (Charmandari et al., 2005; Nicolaides et al., 2015). The

stress-induced GC production facilitates stress coping and allows the control of circulating levels of the steroid to return to basal levels, both mediated by activating either the glucocorticoid receptor (Gr) and/or the mineralocorticoid receptor (Mr) (Charmandari et al., 2005; De Kloet et al., 1998; Nicolaides et al., 2015).

The critical role of Pomc in adrenal function is evident from studies showing that mutations in Pomc lead to adrenal insufficiency and a loss of stress-induced GC elevation (Charmandari et al., 2014). To a large extent, the circulating GC levels dictate the activation of the corticosteroid receptors, as Mr has a 10 x higher affinity for this steroid and hence basal levels of GCs bind to Mr, whereas stress-induced and/or circadian peak in this steroid preferentially activates the Gr (De Kloet et al., 1998, 2018). Pomc mutations, which disrupt the Acth and α-Msh peptide synthesis, have been associated with early developmental adrenal insufficiency, lack of GC response to stress, obesity, and abnormal pigmentation in human patients (Krude & Grüters, 2000; Krude et al., 1998). The obesity in Pomc mutants is primarily associated with a dysfunction in the central melanocortin system (Kühnen et al., 2019; Sweeney et al., 2023), as the central Pomc-derived α-Msh is an agonist of the melanocortin 4 receptor (Mc4r) and suppresses feeding (anorexigenic). The lack of α-Msh in the Pomc mutants lead to an upregulation in the orexigenic peptide agouti-related protein (Agrp), which stimulates hyperphagia and obesity (Sweeney et al., 2023; Zhang et al., 2012).

While the role of hypothalamic-melanocortin system in the etiology of childhood obesity has received attention (Farooqi et al., 2000; Krude & Grüters, 2000; Kühnen et al., 2019), an understanding of the contribution of peripheral signaling to increased adiposity in the Pomc mutants is lacking. Given that basal GC levels preferentially activate Mr (De Kloet et al., 1998, 2018), a key stimulator of postnatal adipogenesis in mammals and zebrafish (*Danio rerio*) (Caprio et al., 2007; Faught & Vijayan, 2019), we tested the hypothesis that Pomc mutation increases adiposity by differentially modulating the corticosteroid receptor signaling using zebrafish as a model. Zebrafish has two paralogs of *pomc* (*pomca* and *pomcb*) (Gonzalez Nunez, 2003), but only *pomca* is functionally relevant for the activation of the hypothalamus-pituitary-interrenal (HPI) axis (Shi et al., 2019), which is analogous to the hypothalamus-pituitary-adrenal (HPA) axis in mammals, as teleosts lack a discrete adrenal gland (Mommsen et al., 1999). Although recent studies confirmed that Pomc knockout showed interrenal insufficiency in zebrafish (Shi et al., 2019; Yang et al., 2023), its role in the development of early adipogenesis has not been addressed. Here we generated a Pomca knockout zebrafish, that mimicked the phenotype exhibited by the Pomc mutants in humans (Krude & Grüters, 2000; Krude et al., 1998), and our results indicate a key role for Mr signaling in mediating the postnatal adiposity.

2 | METHODS

2.1 | Animal care and ethics

Tupfel long fin strain (TL) adult zebrafish were maintained in a re-circulating system (Tecniplast, Italy) that was set to a 14 h light:10 h dark photoperiod, and the water temperature was maintained at 28°C as described previously (Faught & Vijayan, 2018). Fish were fed with dry pellet food in the morning (10:30 AM, Gemma micro-500, Skretting, Canada) and live Artemia culture in the evening (4:00 PM, San Francisco Bay Brand, Inc.). For all experiments, 6–12-month-old male and female zebrafish were used as breeders. For sample collection, the larvae were euthanized with an overdose (4 g/L) of $NaHCO_3$ buffered MS-222 (Tricaine methanesulfonate or TMS, Sigma). All the experiments described in the present study were approved by the Institutional Animal Care Committee (protocol number: AC21-0061) and was in accordance with the guidelines of the Canadian Council for Animal Care.

2.2 | Generation of *pomc*$^{-/-}$ zebrafish

Homozygous mutants lacking *pomca* (*pomc*$^{-/-}$) were generated using CRISPR/Cas9 mutagenesis following the procedure described previously (Faught & Vijayan, 2018). Briefly, wildtype (WT) male and female zebrafish were bred and the embryos at the one-cell stage were injected with the sgRNA: TAATACGACTCACTATAGGAATCCG CCGAAACGCTTCGTTTTAGAGCTAGAAA. Identification of homozygous mutants were carried out as described earlier (Faught & Vijayan, 2018). Briefly, mosaic founders were outcrossed to WT fish. Embryos were collected and DNA was extracted (50 mM NaOH, 20 min at 95°C, and neutralized 1:1 with 100 mM Tris, pH 7.5). Extracted genomic DNA (gDNA) was amplified using site-specific primers (F-gtaaaacgacggccagtCGCAGCCCCTGAACAGATAG, R-gtgt cttCAGGACTTCATGAAGCC-TCC) using the following PCR conditions: 95°C (5 min), 40 cycles of 94°C (1 min), 57°C (1 min), 72°C (30 s), final extension at 72°C (5 min), hold at 4°C. The PCR products were sent for Sanger sequencing and analyzed using the Seq Scanner 2 Software (Applied Biosystems) to identify the mosaic founders. Heterozygous fish were incrossed and WT, heterozygous, and homozygous mutants were confirmed via capillary electrophoresis fragment analysis (University of Calgary, Sequencing Core Facility). In all cases, we used maternal zygotic mutants (incross of Pomca KO (*pomc*$^{-/-}$) siblings).

2.3 | Functional knockout confirmation

To check if the mutants generated were a functional knockout, we performed the following tests.

2.3.1 | Immunohistochemical localization of Acth and α-Msh

The *pomc*$^{-/-}$ larvae were subjected to immunohistochemistry (IHC) to confirm the loss of Acth and α-Msh following histological techniques as described earlier (Santos et al., 2008). The sections were incubated with anti-Acth (ab74976, Abcam, rabbit polyclonal, 1:100) and anti-α-Msh (ab123811, Abcam, rabbit polyclonal, 1:100) antibodies in a humid chamber overnight at 4°C, followed by secondary antibody (anti-rabbit

Alexa Fluor 488, 1:500) solution for 2 h at room temperature. The nucleus was stained using DAPI. Slides that did not receive the primary antibody were run as a negative control. Both the anti-Acth and anti-α-Msh primary antibodies have been previously validated in fish (Royan et al., 2021). The slides were imaged immediately with a Leica DFC 345 FX fluorescent camera (Leica Microsystems). Zebrafish brain atlas (https://zfin.org/zf_info/anatomy.html) was used as reference to identify the different regions of the brain.

2.3.2 | Pigmentation

To assess the pigmentation, both WT and *pomc*$^{-/-}$ larvae at 6 dpf were euthanized (MS-222) and imaged immediately using a M165 Dissecting Scope (Leica). The pigment intensity was quantified in the head region (between the eye and trunk as shown in Figure 1c) using ImageJ (NIH) as described previously (Balamurugan et al., 2022).

2.3.3 | Stress-induced cortisol response

To assess stress-induced cortisol levels, both WT and *pomc*$^{-/-}$ larvae were subjected to an acute stressor as described previously (Faught & Vijayan, 2018). Briefly, both genotypes were subjected to a physical stressor (swirling stressor; 250 rpm for 1 min, 28°C) and the larvae were euthanized at 5-, 10-, and 30-min post-stressor. A pool of 12 larvae per sample (n = 8–12) were stored at −80°C for cortisol analysis later.

2.4 | Feeding study

Both WT and *pomc*$^{-/-}$ larvae (50 larvae per trial, 4 independent trials) were fed from 6 dpf onwards with Gemma micro 150 (Skretting) with 50% water (zebrafish system water) exchange daily. Equal amounts of feed based on a previous study (Thompson et al., 2024) was provided to each group daily.

2.5 | Hormone and drug treatments

2.5.1 | Cortisol

WT and *pomc*$^{-/-}$ fish at 5 dpf were treated with cortisol (5 ug/mL, hydrocortisone, Sigma) for 16 h, as described previously (Faught & Vijayan, 2022). The next day (6 dpf), larvae were sampled and processed for IHC (brain and liver sectioning for Gr and Mr IHC), transcript abundance and Western blot analysis (see below).

2.5.2 | Eplerenone

To confirm Mr signalling, WT and *pomc*$^{-/-}$ larvae at 5 dpf were treated with the Mr antagonist eplerenone (Sigma) (5 ug/mL) overnight as described previously (Faught & Schaaf, 2023) and the larvae were sampled at 6 dpf for the transcript abundance of Mr-responsive genes. Furthermore, to test whether Mr is mediating the adiposity, both WT and *pomc*$^{-/-}$ larvae were treated with eplerenone (5 ug/mL) from 6 to 15 dpf and growthassessed (see below). Water was replaced (50%) daily with the drug.

2.6 | Growth assessment

Growth assessment was carried out by sampling the larvae at 15 dpf for weight and length, which was obtained by imaging using M165 Dissecting Scope (Leica).

2.7 | Gr and mr immunohistochemistry

To assess the Gr and Mr immunofluorescence in the brain and liver, cross-sections of larvae were obtained as described above. The sections were confirmed by checking under a dissection microscope using ZFIN larval anatomy tool as reference to confirm different areas (https://zfin.org/zf_info/anatomy.html). Following that, the sections were dewaxed and hydrated. Sections were not run through any antigen retrieval protocol for both Gr and Mr antibodies. The rest of the procedure were as described earlier in the IHC section for Acth and α-Msh. Briefly, the sections were treated with 1% SDS in PBS (5 min), followed by blocking with 1% bovine serum albumin (BSA) in PBST (PBS with 0.005% Tween 20) with 5% normal goat serum (20 min). Following blocking, the sections were incubated with the antibodies in a humid chamber overnight at 4°C. The next day, sections were washed with PBST and incubated with secondary antibody (anti-rabbit Alexa Fluor 488, 1:500) for 2 h at room temperature. The nucleus was stained using DAPI. Slides that did not receive the primary antibody were run as a negative control. Both anti-Gr and anti-Mr antibodies were previously validated (Faught & Vijayan, 2018). The slides were imaged with a Leica DFC 345 FX fluorescent camera (Leica Microsystems).

2.8 | Nile red staining

To assess the amount of lipid accumulated in the WT and *pomc*$^{-/-}$ larvae, both groups were subjected to Nile red fluorescent staining as described previously (Thompson et al., 2024). Briefly, WT and *pomc*$^{-/-}$ larvae at 15 dpf were euthanized, incubated with Nile red solution (0.1 µg/mL) for 30 min and imaged immediately with a Leica DFC 345 FX fluorescent camera (Leica Microsystems). The abdominal and subcutaneous lipid accumulating regions including the abdominal visceral (AV), pancreatic visceral (PV), subcutaneous appendicular loose (AL) and abdominal truncal (AT) adipocytes were imaged (Supporting Information S1: Figure S3). ImageJ (NIH) was used for quantifying the fluorescent intensity or relative fluorescence units (RFU) as described previously (Balamurugan et al., 2022; Thompson et al., 2024).

2.9 | Western blot

Sodium dodecyl sulfate–polyacrylamide gel electrophoresis (SDS-PAGE) and Western blot analysis for zebrafish Gr and Mr were performed as described previously (Faught & Vijayan, 2018). The membranes were probed with either anti-trout Gr (1:1000) or anti-zebrafish Mr (1:500) primary antibodies overnight at 4°C followed by goat anti-rabbit IgG secondary antibody (1:2000; Bio-Rad) for 2 h at

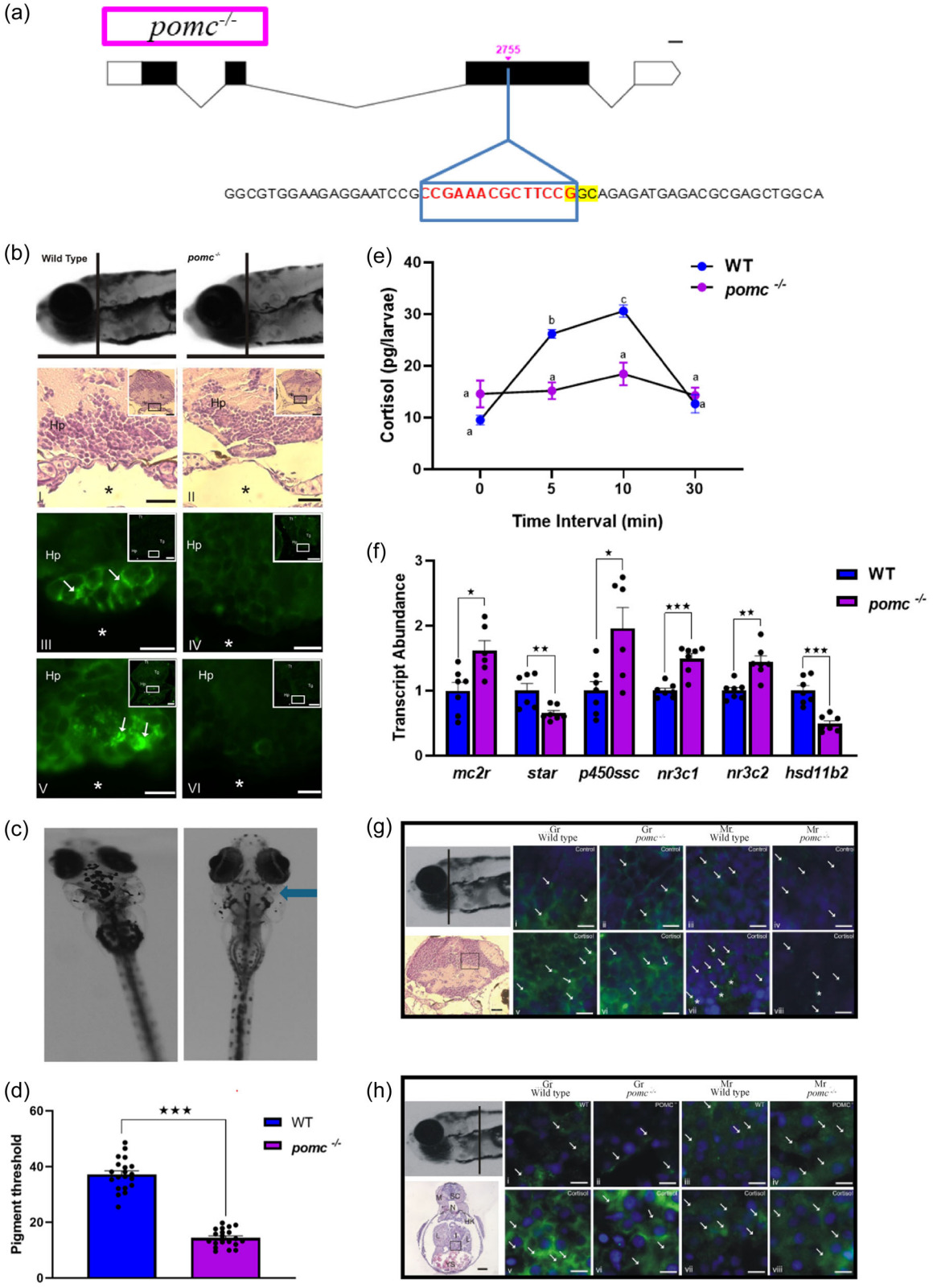

FIGURE 1 (See caption on next page).

room temperature as described previously (Faught & Vijayan, 2018). The image of the full blot is shown in Supporting Information S1: Figure S2.

2.10 | Triglyceride and glycerol measurement

The samples were homogenized as mentioned above and the triglyceride and glycerol concentrations were measured using a commercial kit (Sigma) as described previously (Faught & Vijayan, 2019; Thompson et al., 2024).

2.11 | RNA extraction, cDNA synthesis and qPCR

WT and *pomc*$^{-/-}$ larvae at 6 and 15 dpf were euthanized using an overdose of MS-222 and were flash frozen on dry ice and stored at −80°C. TRIzol reagent (Invitrogen) was used for total RNA extraction following the manufacturer's instructions. The quality and quantity of the extracted RNA (260/280 and 260/230 ratios) were measured using a Nanodrop 2000 spectrophotometer (Thermo Scientific). A total of 1 µg RNA was treated with DNase I (Thermo Scientific), followed by cDNA synthesis using High-Capacity cDNA reverse transcription kit (Applied Biosystems) following manufacturer's instruction. SS Advanced SYBR green (Bio-Rad) and QuantStudio 3 Real-Time PCR system (Applied Biosystems) was used for quantifying transcript abundance. The forward and reverse sequence of the primers used for qPCR are shown in Table 1. The qPCR cycle conditions used were: 94°C for 2 min, followed by 40 cycles at 95°C for 30 s, primer-specific annealing temperatures for 30 s, and 10 min at 72°C. For data normalization, b-actin was run as the housekeeping reference genes. Primer validation (via Sanger sequencing), and optimization were carried out before qPCR. To verify the absence of primer dimers or artifacts for each primer set, a melt curve analysis (65°C to 95°C (5 s) was performed for each run. All samples were run in duplicates and negative controls (nuclease-free water instead of cDNA) were run for each gene. Data were analysed and the relative transcript abundance was assessed using the $2^{-\Delta\Delta CT}$ method as described previously (Thompson et al., 2024). All transcripts shown in the manuscript are from cDNA obtained from larval total RNA.

2.12 | Statistical analysis

For comparing two groups, Student's *t* test was used, while for multiple comparisons, one-way ANOVA followed by Tukey's post hoc test was carried out and $p < 0.05$ was considered significant. Whole larval cortisol data were analyzed using two-way ANOVA followed by Tukey's multiple comparison test ($p < 0.05$). PRISM version 7 (GraphPad Inc.) software was used for statistical analysis and for generating graphs. All data are represented as mean + SEM with overlayed data points (in bar graphs). Data sets that failed to meet the assumptions of normality and homoscedasticity were transformed before statistical analysis, but all data sets shown in the graphs are untransformed data.

3 | RESULTS

3.1 | Lack of pomca reflects interrenal insufficiency

As the lack of Pomca led to interrenal insufficiency in zebrafish (Shi et al., 2019), we edited *pomca* (*pomc*$^{-/-}$) at exon 3 by CRISPR/Cas9 mutagenesis to generate a knockout (Figure 1a and Supporting

FIGURE 1 Lack of Pomca reflects interrenal insufficiency. (a) Schematics of the Pomca knockout (*pomc*$^{-/-}$) showing the 14 bp deletion (red letters) in the exon 3 of the Pomca gene. The white box on either end represents the 5′−3′ upstream and downstream sequences, respectively, and the introns are represented as black lines and exons as a black box; (b) Anatomical view of wildtype, and *pomc*$^{-/-}$ larvae at 6 days post-fertilization (dpf) showing where the histological sections were obtained for identification of the hypothalamus and pituitary regions. The top panel shows the cross-section of brains stained with hematoxylin and eosin (I and II) and the bottom panels are immunostained for Acth (III and IV) and a-Msh (V and VI); Tectum (Tt), tegmentum (Tg) and hypothalamus (Hp). White arrows indicate Acth- and a-Msh-positive cells. Asterisk (*) denotes the cranial cavity. The rectangle in the insert indicates the hypothalamic and pituitary regions that were magnified. I–II (bar 20 µm), III–VI (bar 10 µm) and Insert (bars 40 µm). The Acth and a-Msh immunoreactivity is absent in the *pomc*$^{-/-}$ larvae; (c) Representative image of 6 dpf larva showing reduced pigmentation in the *pomc*$^{-/-}$ larvae (arrowhead) compared to WT (left panel); (d) Quantification of larval pigmentation between the genotypes at 6 dpf (*t* test, $n = 20$ larvae per group, $^{***}p < 0.001$); (e)The acute cortisol response to a physical stressor (1 min at 250 rpm) was inhibited in the 4 dpf *pomc*$^{-/-}$ larvae (symbols with different letters are significantly different (2-way ANOVA; $n = 8–12$, each a pool of 12 larvae); (f) bars represent significant differences in the transcript abundance of *mc2r*, *star*, *p450ssc*, *nr3c1*, *nr3c2*, and *hsd11b2* in WT and *pomc*$^{-/-}$ larvae at 6 dpf (*t* test, $n = 6–7$, each a pool of 12 larvae, $^{*}p < 0.05$, $^{**}p < 0.01$, $^{***}p < 0.001$); (g) Anatomical view of wildtype and *pomc*$^{-/-}$ larvae at 6 dpf showing glucocorticoid receptor (Gr) and mineralocorticoid receptor (Mr) immunoreactivity in the control (i and iii and ii and iv) and cortisol (v and vii and vi and viii) treated groups in the hypothalamus. The panel on the left side shows the anatomy and cross-section of the body stained with Hematoxylin and Eosin (H&E) and the area inside the box indicate where the zoomed images of the brain were acquired to evaluate the immunostaining for Gr and Mr expression (white arrows and *); (h) Cross-section of WT (i, iii, v and vii) and *pomc*$^{-/-}$ (ii, iv, vi and viii) larvae liver at 6 dpf showing Gr and Mr immunoreactivity with and without cortisol treatment. The panel on the left side shows the anatomy and cross-section of the body stained with H&E to indicate where the zoomed images of the liver were acquired to evaluate the immunostaining for Gr and Mr expression; white arrows indicate Gr- and Mr-positive hepatocytes; spinal cord (SC), notochord (N), muscles (M), head kidney (HK), anterior intestine (I), yolk sac (YS) and liver (L). Bars: 10 µm (i–viii) and 50 µm for the trunk stained with H&E. The transcript abundance and cortisol levels are from whole larvae.

TABLE 1 List of primers used for qPCR.

Gene name	Accession number	Forward primer (5′–3′)	Reverse primer (5′–3′)
β-actin	NM_181601 2	TGTCCCTGTATGCCTCTGGT	AAGTCCAGACGGAGGATG
nr3c1	NM_001020711.3	ACAGCTTCTTCCAGCCTCAG	CCGGTGTTCTCCTGTTTGAT
nr3c2	NM_001100403.1	CCCATTGAGGACCAAATAC	AGTAGAGCATTTGGGCGTTG
igf1	NM_131825.2	CCACGATCTCTACGAGCACA	TCGGCTCGAGTTCTTCTGAT
igf2	NM_001001815.1	TGCAGGTCATTCCAGTGATG	TAGCCTCTGAGCAGCCTTTC
igf1ra	NM_152968.1	GTTTGACGAGACGCAGCCTTAC	CAAAGGGAGGAGGGAAATGTGT
igf1rb	NM_152969.1	CGGATGCGTCGGATGTGTGT	GTCTGGCGGAAATAACAAATGAGT
igf2r	NM_001039627.2	ACCCCTGTCCTCAAGTAACAGAT	TTGCACACCGTCAGTACAAAAG
lpl	NM_131127.1	ACAATTGACCCAACTGCTGA	GGTTCTTCGAGGGTCCGAAA
fasn	XM_056470098.1	GGAGCAGGCTGCCTCTGTGC	TTGCGGCCTGTCCCACTCCT
elovl2	NM_001040362.1	CACTGGACGAAGTTGGTGAA	TTGAGGACACACCACCAGA
dgat2	NM_001030196.1	CCATACTTGCTGCATATTCC	ATGTCATGATAAACTGCAGC
pparγ	NM_131467.1	TGCCGCATACACAAGAAGAG	ATGTGGTTCACGTCACTGGA
fkbp5	NM_213149.1	GTGTTCGTCCACTACACC	TCTCCTCACGATCCCACC
hsd11b2	NM_212720.2	TGCTGCTGGCTGTACTTCAC	ATCCAACTTCTTTGCTG
Lepa	NM_001128576.1	TCGTCAGAATCAGGGAACAC	CCCAATGATGAGCGTTGGA
Lepb	NM_001030186.3	GATGAGCACTTCCAGATGTC	TGTCTATGTTGAGGCAGAGC
Crh	NM_001007379	CACCGCCGTATGAATGTAGA	GAAGTACTCCTCCCCCAAGC
crhr1	XM_056453349.1	CAGTCATCATCAACTACCTGGG	AGCTGAACCACGAACCA
mc2r	NM_180971.1	CTCCGTTCTCCCTTCATCTG	ATTGCCGGATCAATAACAGC
mc3r	NM_180972	CTGATTCTCCAGCAGGGACG	ACCACAGCCGAGATGACAAG
mc4r	NM_173278	AGCCCTCTCATGGTGACAGA	CGATGGCTGCAATCACAAGG
Star	NM_131663.1	TCAAATTGTGTGCTGGCATT	CCAAGTGCTAGCTCCAGGTC
p450ssc	NM_152953	AGGGCCATCACCCCAATAG	CCAGGCCTTCCCTTCTTTTAG
Agrp	NM_001328012.1	CACAGACTCACTGCCTGAAA	TAGCCTCTGAGCAGCCTTTC
npy	NM_131074.2	CAAGCGCTGACACCTTAAT	GATGAGATCACCATGCCAAATG

Information S1: Figure S1). The homozygous mutants lacked Acth and α-Msh immunoreactivity in the pituitary gland of zebrafish larvae (Figure 1b). The mutant larvae also showed hypopigmentation compared to the WT larvae (Figure 1c,d). Furthermore, the *pomc*$^{-/-}$ larvae were unable to elicit an acute stress-induced cortisol elevation (Figure 1e), which was evident in the wildtype larvae with a functional HPI axis (Alsop & Vijayan, 2008; Faught & Vijayan, 2018), confirming a secondary interrenal insufficiency. Among the HPI axis-related genes we tested, *mc2r*, *p450ssc*, *nr3c1* and nr*3c2* transcripts were significantly higher, whereas *star*, and *hsd11b2* were significantly lower in the *pomc*$^{-/-}$ group compared to the WT larvae (Figure 1f). The target tissue Gr and Mr immunoreactivity in the brain and liver remained unchanged in both genotypes (Figure 1g,h). As teleosts lack aldosterone, it has been shown that cortisol acts both as a GC and a mineralocorticoid (Baker & Katsu, 2017; Kiilerich et al., 2011; McCormick et al., 2008). So, we tested whether cortisol stimulation modulated the corticosteroid receptor expression in the Pomc mutants. Indeed, treating larvae with cortisol led to an increase in the Gr and Mr immunoreactivity in the brain (Figure 1g) and liver (Figure 1h), irrespective of the genotype.

3.2 | Lack of pomc increases postnatal Mr responsiveness

To test if the loss of *pomca* affects corticosteroid receptor responsiveness, we assessed Gr and Mr protein expression and their target genes response in the unstimulated and cortisol-stimulated WT and Pomc mutants. As seen with the IHC, the whole larvae Gr (Figure 2a) and Mr (Figure 2b) unstimulated protein expression did not show a

genotype effect. However, cortisol stimulated the corticosteroid receptor protein expression in both genotypes. The Gr protein expression was lower (Figure 2a), whereas the Mr protein expression was higher (Figure 2b) in the *pomc*$^{-/-}$ larvae compared to the wildtype, suggesting a possible genotype-specific differential corticosteroid receptor activation. To test this, we measured the transcript abundance of their target genes in zebrafish. Previous studies have shown that the leptin paralogs (*lepa* and *lepb*) are an excellent readout for Mr activation, along with *fkbp5* and *11bhsd2* as readouts for Gr activation in zebrafish larvae (Faught & Vijayan, 2019, 2020; Gans

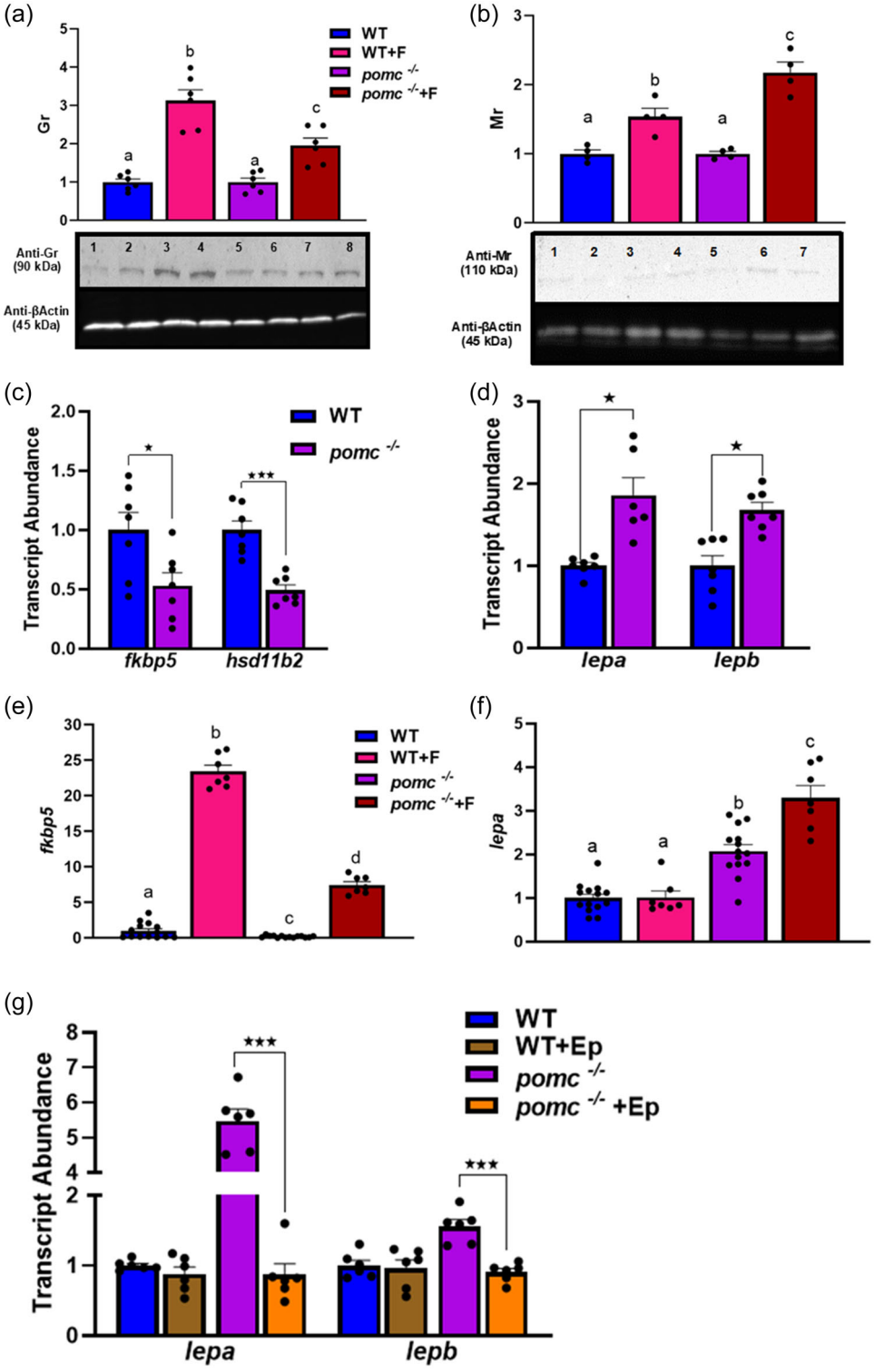

FIGURE 2 (See caption on next page).

et al., 2021). Despite the absence of any change in the corticosteroid receptor protein expression between the genotypes, the transcript abundance of *fkbp5* and *11bhsd2* were lower (Figure 2c) whereas the *lepa* and *lepb* were higher (Figure 2d) in the *pomc*$^{-/-}$ larvae confirming differential receptor responsivity. This was further evident in the cortisol-stimulated larvae, where the higher receptor protein expression reflected a higher transcript abundance of their respective responsive genes. However, the cortisol-induced *fkbp5* gene expression was attenuated (Figure 2e), whereas the cortisol-induced *lepa* gene expression was strengthened (Figure 2f) in the *pomc*$^{-/-}$ larvae compared to the WT, pointing to a reduced Gr- and enhanced Mr-responsiveness. So, to confirm if indeed the upregulation of *lep* paralogs were due to Mr signaling, we treated the larvae with eplerenone, a Mr-specific antagonist in zebrafish (Faught & Schaaf, 2023; Pippal et al., 2011). Eplerenone abolished the *lepa* and *lepb* upregulation (Figure 2g) in the *pomc*$^{-/-}$ zebrafish larvae.

3.3 | Lack of pomca enhances postnatal growth

As early onset childhood obesity is a hallmark of the Pomc mutants, we investigated whether enhanced postnatal growth was also the case in our zebrafish model. For this, we assessed growth and lipid accumulation 9 days (at 15 dpf) after the commencement of larval feeding as described previously (Faught & Vijayan, 2019). Both genotypes had similar basal cortisol levels at 15 dpf (Figure 3a), but the *pomc*$^{-/-}$ larvae were longer (Figures 3b,c) and 50% heavier (Figure 3d) post-feeding. We measured the feeding-related peptide to assess whether the heavier body mass may be associated with hyperphagia. There were no significant changes in the transcript abundance of orexigenic neuropeptides *agrp* and *npy* (Figure 3e), while the transcript abundance of key melanocortin receptors, including *mc3r* and *mc4r*, involved in feeding suppression was higher in the *pomc*$^{-/-}$ larvae (Figure 3e). Also, we did not observe any significant changes in either the total protein content (Figure 3f) or genes (Figure 3g) involved in regulating the lean body mass, including the *igfs* and their receptors (Wood et al., 2005), leading us to the hypothesis that the higher larval mass in the Pomc mutants may be due to enhanced lipid accumulation.

3.4 | Lack of pomca enhances postnatal adiposity

We tested for increased adiposity in these mutants by using a combination of Nile red imaging, metabolite measurement and transcript abundance of adipogenic genes post-feeding. The lack of Pomc increased the overall lipid droplet accumulation in the visceral (abdominal and pancreatic visceral) and subcutaneous (appendicular and abdominal truncal) adipocytes (Figure 4a). This was also accompanied by elevated triglyceride (Figure 4b) and glycerol levels (Figure 4c) in the *pomc*$^{-/-}$ larvae compared to the WT. Furthermore, the corresponding regulation of key genes involved in adipogenesis, including the upregulation of *fasn* and *pparg* and the downregulation of the lipolytic gene *lpl* (Figure 4d), indicate a developmental programming effect favoring postnatal adiposity in the *pomc*$^{-/-}$ fish.

3.5 | Lack of pomc-induced adiposity is mr-mediated

Consequently, we tested whether the increased adiposity seen in the *pomc* mutants is due to enhanced Mr responsiveness. We tested this by treating the larvae with eplerenone (Ep) during the feeding period with the prediction that the Mr antagonist would inhibit the *pomc*$^{-/-}$-induced body mass gain and lipid accumulation. Our WT and *pomc*$^{-/-}$ responses were like that observed previously in the absence of eplerenone (Figures 2d,g, 3c,d, and 4b–d), so we are showing the results as % change from control (WT and *pomc*$^{-/-}$). Eplerenone treatment during the 9 days of feeding resulted in no change in the *lepa* and *lepb* transcript abundance in larvae lacking Pomca (Figure 5a), whereas in the absence of the Mr antagonist, there was an upregulation in *lepa* and *lepb* in the *pomc*$^{-/-}$ fish (Figure 2d,g).

FIGURE 2 Lack of Pomca increases postnatal mineralocorticoid receptor (Mr) responsiveness. (a) Representative Western blot of 6 dpf larvae showing glucocorticoid receptor (Gr) protein expression (~90 kDa: lanes 1–2 WT, lanes 3–4 WT + F (cortisol), lanes 5–6 *pomc*$^{-/-}$, Lanes 7–8 *pomc*$^{-/-}$ + F). The original unprocessed blot images are shown in the supplemental file (Supporting Information S1: Figure S2). The lower blot shows b-actin expression as a loading control. The bar graph below represents the semi-quantitative image of the Gr band intensity ($n = 6$, each a pool of 12 larvae, bars with different letters are significantly different, one-way ANOVA, $p < 0.05$); (b) Representative Western blot of 6 dpf larvae showing Mr protein expression (~110 kDa: lane 1 WT, lanes 2–3 WT + F, lanes 4–5 *pomc*$^{-/-}$, lanes 6–7 *pomc*$^{-/-}$ + F). The lower blot shows β-actin expression as a loading control. The bar graph shows below represents the semi-quantitative image of the Mr band intensity ($n = 4$, each a pool of 12 larvae, bars with different letters are significantly different, one-way ANOVA, $p < 0.05$); (c) Shows the transcript abundance of Gr-responsive genes, *fkbp5* and *hsd11b2* in 6 dpf WT and *pomc*$^{-/-}$ larvae. Bars with asterisk (*) are significantly different (*t* test, $^{*}p < 0.05$ and $^{***}p < 0.001$, $n = 6–7$, each a pool of 12 larvae); (d) Represent the transcript abundance of Mr-responsive genes, *lepa* and *lepb* in 6 dpf WT and *pomc*$^{-/-}$ larvae. Bars with asterisk (*) are significantly different (*t* test, $^{*}p < 0.05$, $n = 6$-7, each a pool of 12 larvae); (e) Shows the transcript abundance of Gr-responsive gene *fkbp5* either without or with cortisol (F) and (f) Shows the transcript abundance of Mr-responsive gene *lepa* either without or with cortisol (F) in 6 dpf WT and *pomc*$^{-/-}$ larvae; bars with different letters are significantly different (one-way ANOVA, $p < 0.05$, $n = 7–14$, each a pool of 12 larvae); (g) Shows the transcript abundance of Mr-responsive genes, *lepa* and *lepb* following eplerenone (Ep) treatment in WT and *pomc*$^{-/-}$ fish at 6 dpf (*t* test, $n = 5–7$, each a pool of 5–8 larvae, $^{***}p < 0.001$). The transcript abundance and Western blot results are from the whole larvae.

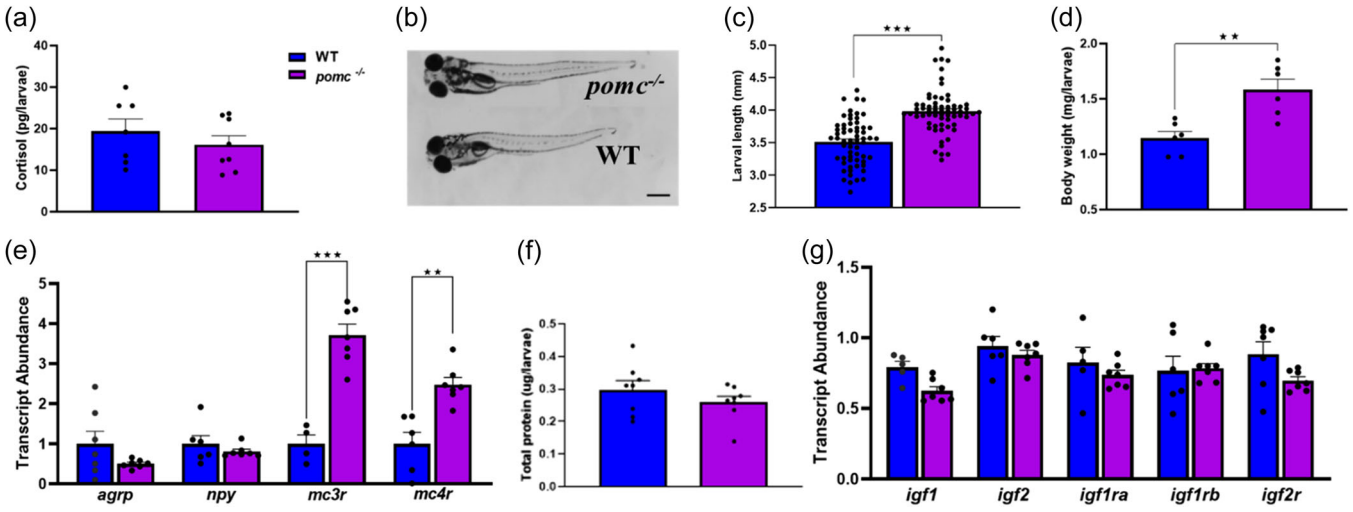

FIGURE 3 Lack of Pomca enhances postnatal growth. (a) No significant changes in total cortisol were observed between WT and KO groups at 15 dpf (n = 7–8, each a pool of 6–8 larvae); (b) Representative images of the WT and *pomc*$^{-/-}$ larvae showing the difference in length at 15 dpf (bar is 0.20 mm; (c) Bars represent significant increase in larval length in the *pomc*$^{-/-}$ larvae compared to WT at 15 dpf (n = 60–66 individual larvae, t test, ***p < 0.001); (d) Larval weight at 15 dpf were higher among the *pomc*$^{-/-}$ fish compared to WT (n = 6, each a pool of 4 to 8 larvae, t test, **p < 0.001); (e) Graph showing the transcript abundance of feeding regulatory transcripts, including *agrp*, *npy*, *mc3r* and *mc4r* in WT and KO larvae at 15 dpf. Significant differences between the two groups (t test, n = 5–7, each a pool of 5–8 larvae, **p < 0.01, ***p < 0.001); (f) No significant changes in the total protein content between WT and *pomc*$^{-/-}$ larvae at 15 dpf (n = 8, each n composed of 6–8 larvae per group); G) Transcript abundance of *igf1*, *igf2*, *igf1ra*, *igf1rb* and *igf2r* were not affected by Pomca loss in zebrafish larvae (n = 5–7, each a pool of 5–8 larvae. The transcript abundance, cortisol, body weight and total protein levels are from whole larvae.

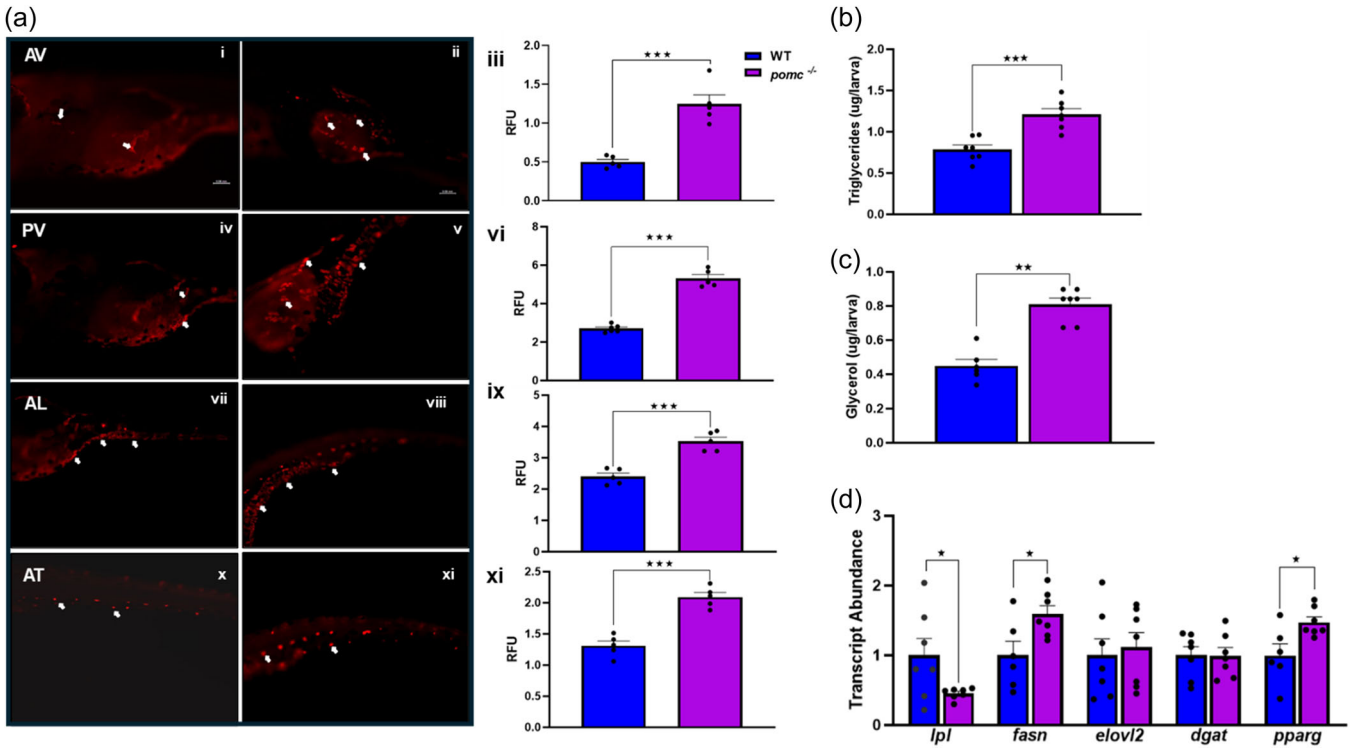

FIGURE 4 Lack of Pomca enhances postnatal adiposity. (a) Nile red staining shows lipid deposition in different regions, including abdominal visceral (AV; i and ii), pancreatic visceral (PV; iv and v), appendicular loose (AL; vii and viii), and abdominal truncal (AT; x and xi) in the 15 dpf WT and *pomc*$^{-/-}$ larvae, and the corresponding quantification as relative fluorescence units (RFU) are shown as histogram next to the panels (iii, vi, ix, and xii; t test, n = 5–6 larvae; ***p < 0.001); (b) bar graph represent triglyceride levels at 15 dpf in WT and *pomc*$^{-/-}$ larvae (n = 7, each a pool of 8–12 larvae; t test, ***p < 0.001); (c) Glycerol levels are elevated in the 15 dpf *pomc*$^{-/-}$ larvae compared to the WT larvae (n = 7, each a pool of 8–12 larvae; t test, **p < 0.01); (d) Shows the transcript abundance of *lpl*, *fasn*, *elovl2*, *dgat*, and *pparg* at 15 dpf in the *pomc*$^{-/-}$ and WT larvae; significant difference between the two groups (t test) are shown as *p < 0.05. The transcript abundance and metabolite levels are from whole larvae.

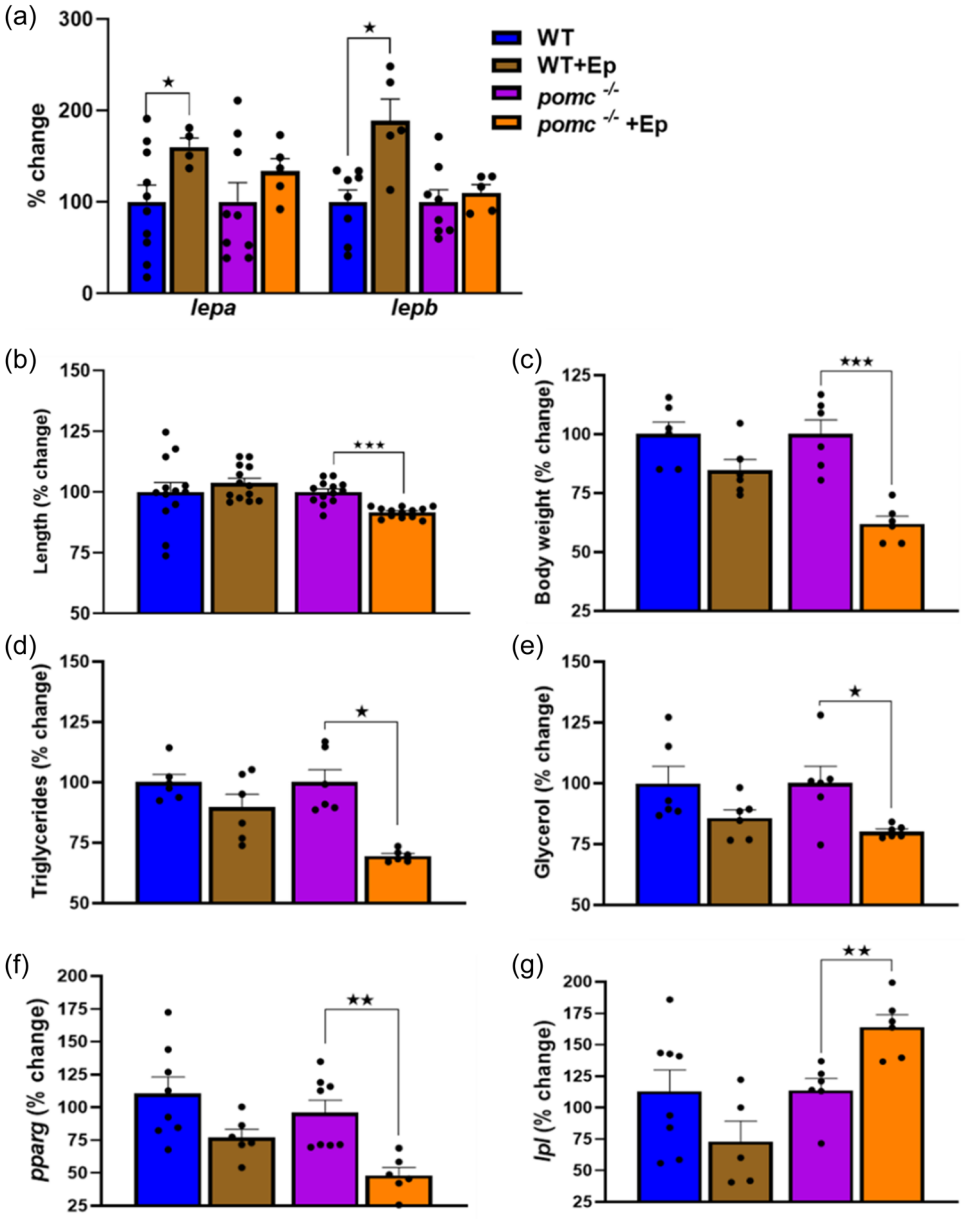

FIGURE 5 Pomc-induced adiposity is mineralocorticoid receptor (Mr) mediated. To test if the adiposity phenotype in *pomc*$^{-/-}$ larvae is due to enhanced Mr responsiveness, both WT and *pomc*$^{-/-}$ larvae were treated with eplerenone (Ep) for 9 days (5 µg/mL; replenished 50% daily) from day 6 and sampled at 15 dpf. The WT and *pomc*$^{-/-}$ without Ep were set as 100% to indicate the percent change due to Ep treatment in both the genotypes. (a) Bar graph showing percent change in the transcript abundance of *lepa* and *lepb* following Ep treatment in WT and *pomc*$^{-/-}$ larvae (*t* test, $n = 4–7$, each a pool of 5–8 larvae, $^{*}p < 0.05$); (b) Shows the percent change in length following Ep treatment for 9 days (*t* test, $n = 15–24$ larvae; $^{***}p < 0.0001$); (c) Represent percent change in body weight in both WT and *pomc*$^{-/-}$ larvae following Ep treatment (*t* test, $n = 6$, 5–7 larvae per group; $^{***}p < 0.0001$); (d) Shows the percent change in total triglycerides post Ep treatment in WT and *pomc*$^{-/-}$ larvae at 15 dpf (*t* test, $n = 6$, 5–7 larvae per group; $^{*}p < 0.05$); (e) Bars represent the percent change in whole larval glycerol content in WT and *pomc*$^{-/-}$ larvae at 15 dpf following a 9 day Ep treatment (*t* test, $n = 6$, 5–7 larvae per group; $^{*}p < 0.05$); (f) Percentage change in the transcript abundance of *pparg* following Ep treatment ($n = 6–7$, each a pool of 5–7 larvae, $^{**}p < 0.001$); (g) Percentage change in the transcript abundance of *lpl* following Ep treatment ($n = 6–7$, each a pool of 5–7 larvae, $^{**}p < 0.001$). The transcript abundance and metabolite changes are from the whole larvae.

Furthermore, while a loss of Pomca resulted in an increase in the larval length (Figure 3c) and mass (Figure 3d), there was a reduction in larval length (Figure 5b) and mass (Figure 5c) in *pomc*$^{-/-}$ larvae treated with eplerenone. To test whether the enhanced growth seen in the *pomc*$^{-/-}$ fish was due to Mr effect on lipid accumulation, we treated the *pomc*$^{-/-}$ fish with eplerenone and assessed the triglyceride and glycerol levels as well as the transcript abundance of target genes involved in adipogenesis. Similar to the above results, treatment of *pomc*$^{-/-}$ fish with eplerenone resulted in a lowering of triglyceride (Figure 5d) and glycerol levels (Figure 5e), whereas both these

metabolites were higher in the larvae lacking Pomca in the absence of eplerenone (Figure 4b-c). Also, changes in the molecular markers of adipogenesis, including downregulation of *pparg* (Figure 5f), and upregulation of *lpl* (Figure 5g) with eplerenone in the *pomc*$^{-/-}$ larvae points to a developmental programming effect of Mr activation on lipid synthesis.

4 | DISCUSSION

Our results underscore the key role of stress axis activity in regulating peripheral control of adiposity in zebrafish larvae. The lack of Acth and the associated inactivity of the stress-induced cortisol production in the Pomc mutants reprogram corticosteroid signaling to promote postnatal adiposity in larval zebrafish (Figure 6). Indeed, Mr activation by cortisol has been shown to increase adipogenesis and lead to obesity in mammalian models (Hulse et al., 2022; Parasiliti-Caprino et al., 2022) and also to increase lipid accumulation in postnatal zebrafish (Faught & Vijayan, 2019). Thus, the enhanced Mr responsiveness of the Pomca mutants played a role in the postnatal adiposity seen in the zebrafish larvae, as this response was completely abolished by Mr antagonism. Although most studies have associated Pomc mutations and the associated early-onset childhood obesity with central dysregulation of the melanocortin four receptor system (Farooqi et al., 2000; Krude & Grüters, 2000; Kühnen et al., 2019) our results underscore Mr activation as a novel peripheral signal contributing to postnatal adiposity in zebrafish lacking Pomc.

Emerging evidence supports the utility of zebrafish as an excellent model for obesity and other metabolic disorders (Faillaci et al., 2018; Zang et al., 2018), and our Pomca knockout zebrafish mimics the early-onset adiposity phenotype seen in humans (Baker et al., 2005; Krude et al., 1998; Kühnen et al., 2019). We generated the Pomca knockout (*pomc*$^{-/-}$) using CRISPR/Cas9 gene editing resulting in a 14 base pair deletion of *pomca* gene. Previous studies have confirmed that Pomca and not Pomcb contribute to the activation of the HPI axis (Kwan et al., 2016; To et al., 2007), and this was

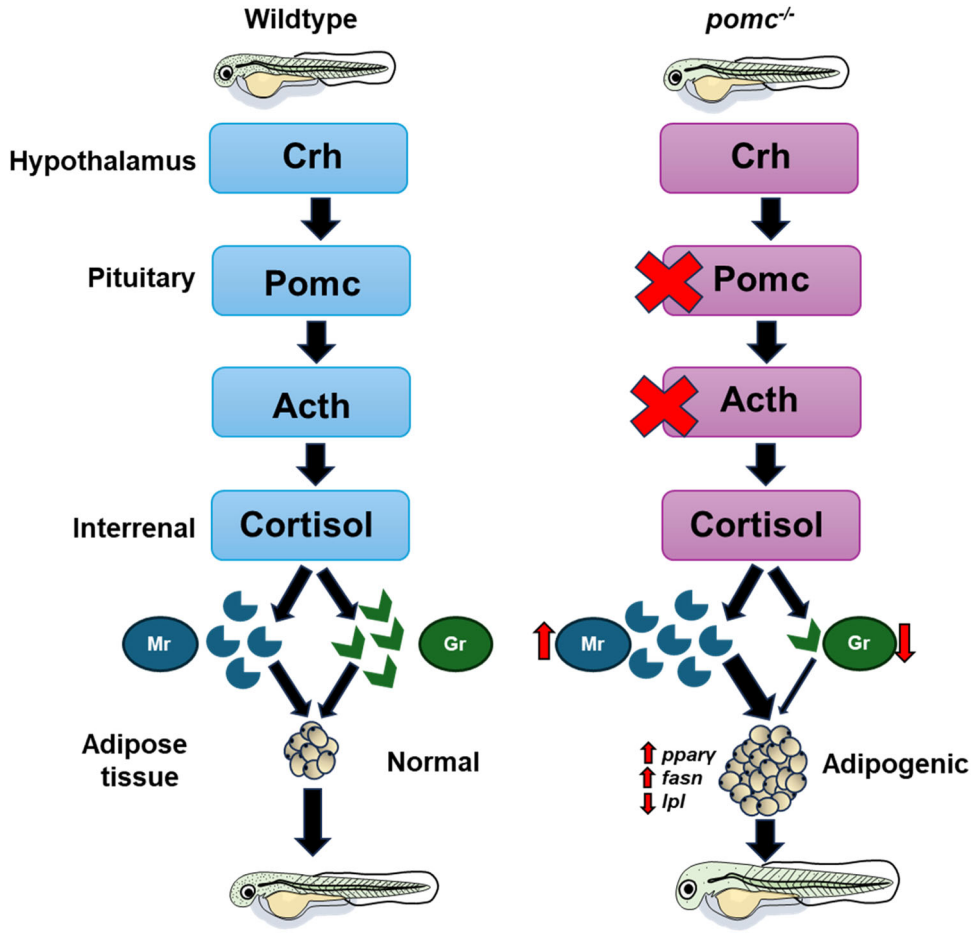

FIGURE 6 Schematic representation of Mr activation as a possible peripheral mechanism leading to adiposity in Pomc mutants. The left panel shows the hypothalamus-pituitary-interrenal (HPI) axis function in the wildtype larvae leading to normal growth post-feeding. The right panel shows that the loss of Pomc leads to a lack of Acth and this leads to a reduced Gr responsiveness and an enhanced Mr responsiveness, which regulates adipogenic genes, including *pparg*, *lpl* and *fasn*, leading to adiposity. Acth, Adrenocorticotropic hormone; Crh, Corticotropin-releasing hormone; *fasn*, Fatty acid synthase; Gr, Glucocorticoid receptor; *lpl*, Lipoprotein lipase; Mr, Mineralocorticoid receptor; Pomc, Proopiomelanocortin; *ppary*, Peroxisome proliferator-activated receptor gamma.

supported by the *pomca*$^{-/-}$ that lacked a stress-induced cortisol response in zebrafish (Shi et al., 2019; Yang et al., 2023). We generated maternal-zygotic mutants to limit the effects of maternally derived-mRNA from heterozygous mothers (Faught & Vijayan, 2018), and the loss-of-function was confirmed by multiple endpoints. Our *pomc*$^{-/-}$ was functional, as IHC revealed the complete loss of both Acth and α-Msh immunoreactivity in the pituitary gland of the zebrafish larvae. The functional relevance of the knockout was further supported by a significant reduction in the pigmentation of the larvae (Figure 1c,d), which is associated with a lack of α-Msh production in the pituitary (Shi et al., 2019). Furthermore, the *pomc*$^{-/-}$ larvae were unable to elicit an acute stress-induced cortisol elevation, a response that is seen in the wildtype larvae with a functional HPI axis (Alsop & Vijayan, 2008; Faught & Vijayan, 2018), confirming a secondary interrenal insufficiency due to the Pomc mutation. The lack of changes in the unstressed whole body cortisol levels in the mutants supports the maintenance of basal interrenal steroidogenesis even in the absence of trophic hormones and may include changes in steroid biosynthesis and cortisol catabolism (Ehrhart-Bornstein et al., 1998). The modulation of genes encoding *star* and *p450scc* and the downregulation of *hsd11b2* transcripts (Figure 1f) support changes in cortisol production and catabolism and may have played a role in the maintenance of basal cortisol levels, especially given that whole-body cortisol levels were measured. Despite the lack of change in basal cortisol levels between the genotypes, the transcript abundance of *nr3c1* and *nr3c2* were higher in the mutants, suggesting a possible upregulation of corticosteroid receptor signalling. However, this was not reflected in the Gr and Mr immunoreactivity in the brain (Figure 1g) and liver (Figure 1h) or the larval protein expression (Figure 2a,b) pointing to possible changes in mRNA stability/turnover for the higher transcript abundance in the mutants.

We have previously shown that cortisol treatment affects Gr turnover in the fish liver by modulating the Gr mRNA transcript abundance and protein expression (Sathiyaa & Vijayan, 2003; Vijayan et al., 2003). So, we tested whether there were any differences in corticosteroid receptor responsivity in the WT and *pomc*$^{-/-}$ following cortisol exposure. Interestingly, the cortisol-induced Gr protein expression seen in the WT larvae was reduced in the *pomc*$^{-/-}$, whereas the Mr protein expression was enhanced (Figure 2a,b), indicating a differential regulation of the corticosteroid receptor expression in the *pomc*$^{-/-}$ larvae. A similar differential expression of both Gr and Mr was seen in humans associated with HPA axis dysregulation and adrenal insufficiency (Klok et al., 2011; Medina et al., 2013; Webster et al., 2002), suggesting that the corticosteroid receptor dysregulation associated with adrenal insufficiency may be a conserved response. We tested whether the differential expression of the receptors in the mutants were a reflection of altered receptor responsiveness by measuring the transcript abundance of Gr- and Mr-responsive genes that were validated previously in zebrafish (Faught & Vijayan, 2019, 2020; Gans et al., 2021). Despite the absence of any change in the corticosteroid receptor protein expression between the genotypes, the transcript abundance of Gr-responsive genes *fkbp5* and *11bhsd2* were lower whereas the Mr-responsive genes *lepa* and *lepb* were higher in the *pomc*$^{-/-}$ larvae confirming differential receptor responsivity. This was further evident in the cortisol-stimulated larvae, where the higher receptor protein expression reflected a higher transcript abundance of their respective responsive genes; however, the attenuated cortisol-induced *fkbp5* and the enhancement of cortisol-induced *lepa* gene in the *pomc*$^{-/-}$ larvae compared to the WT, supports a differential activation of the receptors leading to enhanced MR-responsiveness. To confirm that Mr signalling was indeed enhanced in the *pomc*$^{-/-}$ zebrafish, we treated the larvae with eplerenone, a potent Mr antagonist (Faught & Schaaf, 2023; Pippal et al., 2011), which completely abolished the upregulation of *lep* transcripts, confirming an enhanced Mr activation in the *pomc*$^{-/-}$ fish. These results led us to the hypothesis that enhanced Mr activation in the Pomc mutants as a peripheral mechanism stimulating adipogenesis.

Our observed phenotypic changes in the *pomc*$^{-/-}$ zebrafish, including the lack of Acth and cortisol response to stress and abnormal pigmentation, support a conserved phenotype akin to that seen in the human Pomc mutants (Gregoric et al., 2021; Krude & Grüters, 2000; Krude et al., 1998). As early onset childhood obesity is a hallmark of the Pomc mutants, we investigated whether enhanced postnatal adiposity was also the case in our zebrafish model and is associated with enhanced Mr signaling. In this context, we determined the growth of *pomc*$^{-/-}$ after the commencement of feeding from day 6 to day 15 as reported previously (Faught & Vijayan, 2019). The *pomc*$^{-/-}$ larvae were longer and heavier compared to the wildtype at 15 dpf, and this growth phenotype was also seen in juveniles and adult *pomc*$^{-/-}$ zebrafish and corresponded with hyperphagia (Shi et al., 2019; Yang et al., 2023). While we did not measure feed intake, the absence of any changes in the transcript abundance of orexigenic neuropeptides *agrp* and *npy*, and a higher abundance of *mc3r* and *mc4r* in the *pomc*$^{-/-}$ larvae argue against hyperphagia for higher body mass (Soengas et al., 2018). Also, the lack of any significant changes in total protein content or the genes involved in regulating lean body mass, including the *igfs* and their receptors (Wood et al., 2005), all of which were upregulated in the MC4R mutants (Soengas et al., 2018) suggest that the increased body weight is not due to lean body mass in the larval fish in the present study. This led us to the hypothesis that the higher larval mass in the Pomc mutants may involve peripheral control of adipogenesis. To this end, we first tested lipid accumulation using a combination of Nile red imaging, metabolite measurement and transcript abundance of adipogenic genes post-feeding. The lack of Pomc increased the overall lipid droplet accumulation in the visceral and subcutaneous adipocytes indicating enhanced adipogenesis (Elemans et al., 2019; Minchin & Rawls, 2017). This was accompanied by elevated triglyceride and glycerol levels, further supporting adiposity as a contributing factor for the heavier body mass in the *pomc*$^{-/-}$ larvae. The corresponding regulation of the adipogenic genes (Elemans et al., 2019; Faught & Vijayan, 2019; Flynn et al., 2009; Thompson et al., 2024), including the upregulation of *fasn* and *pparg* and the downregulation of the lipolytic gene *lpl*, indicate a developmental programming effect favoring adipogenesis in the *pomc*$^{-/-}$ fish.

Until recently, a physiological role for Mr signaling in teleost was unknown (Baker & Katsu, 2017; Faught & Vijayan, 2018; Sakamoto et al., 2016). The discovery of a physiological role for Mr in zebrafish indicated that cortisol-Mr activation has an anabolic role, including increasing postnatal adiposity (Faught & Vijayan, 2019, 2020). As we observed a differential corticosteroid receptor signaling among the *pomc* $^{-/-}$ zebrafish, we tested if the adipogenesis phenotype that we observed has any association with enhanced Mr responsiveness. To this end, eplerenone treatment completely abolished the adipogenic phenotype that we observed in the *pomc* $^{-/-}$ group. The reduction in body length and weight in the mutants in the presence of eplerenone supports a role for Mr in specifically promoting excess growth in the *pomc* mutant. To test whether this growth was associated with adiposity, we measured changes in triglyceride and glycerol levels, which clearly indicated that the excess mass was associated with Mr-mediated lipid accumulation. Further confirmation of a role for Mr in the *pomc*$^{-/-}$ - mediated adiposity was evident from the regulation of the molecular markers of adipogenesis (Guo et al., 2008; Lefterova et al., 2014; Weinstock et al., 1997), including *pparg*, and *lpl* with eplerenone, pointing to a developmental programming effect of Mr activation on lipid synthesis. Together, these results underscore a key role for Mr signalling in promoting adipogenesis in the Pomc mutants, and the mode of action involves an upregulation in Mr responsiveness.

As the basal cortisol levels preferentially activate Mr due to its higher affinity for the ligand (De Kloet et al., 1998, 2018), our results emphasize an important role for this receptor during early development, where lipid accumulation is essential to support the increased energy demand for rapid growth (Flynn et al., 2009; Quinlivan & Farber, 2017). For instance, there is a critical window during early development when the zebrafish embryo and larvae are hyporesponsive to stress just before the onset of the first feed (Alsop & Vijayan, 2008; Nesan & Vijayan, 2013). We posit that this period may favor basal cortisol-mediated Mr activation in promoting lipid synthesis to support the rapid growth phase that is evident post-first feed. Thus, the GC-Mr signaling may have evolved as an anabolic facilitator to support the early growth trajectory, while the evolution of Gr coincided with a demand for energy substrate mobilization for stress coping and stress recovery (Faught & Vijayan, 2020). Consequently, the differential activation of the two receptors by GCs may play an important role in the modulation of lipid metabolism during early development. The mechanism by which Pomc mutation leads to enhanced Mr responsiveness remains to be elucidated. However, there is some evidence that a loss of Pomc may alter the adrenal corticosteroid profile in mice (Linhart & Majzoub, 2008). For instance, *pomc*$^{-/-}$ mice showed secondary hyperaldosteronism, which was independent of Acth, suggesting that a loss of Pomc may alter the steroid milieu to favor Mr signaling. Although teleosts lack aldosterone, 11 deoxycorticosterone functions as a ligand for Mr activation (Arterbery et al., 2011) and may be modulated by Pomc dysfunction to enhance Mr signaling. Another, possibility may be that the adrenal inactivity due to Pomc dysfunction eliminates the circadian cortisol rhythm, which plays an important role in the regulation of corticosteroid receptor sensitivity (Lightman et al., 2020).

5 | TRANSLATIONAL PERSPECTIVE

From a biomedical perspective, the conserved phenotype we see in our *pomc*$^{-/-}$ model to the human Pomc mutants (Krude & Grüters, 2000; Kühnen et al., 2019), provides a tractable model to facilitate potential drug discovery to prevent childhood obesity associated with adrenal insufficiency. While the role of the hypothalamic melanocortin system in the etiology of childhood obesity is well studied (Farooqi et al., 2000), it remains to be seen whether Mc4r and Mr may be acting additively or synergistically to promote adipogenesis. The adipogenic role of Mr appears to be conserved, as mammalian studies have also highlighted the role of Mr in lipid regulation and adiposity (Parasiliti-Caprino et al., 2022). Our finding that eplerenone treatment reduced the early onset adipogenesis in zebrafish larvae underpins Mr as a possible target for therapeutic intervention in early childhood obesity due to Pomc dysfunction and adrenal insufficiency.

AUTHOR CONTRIBUTIONS

Jithine J. Rajeswari Conceptualization, generation and validation of the KO model, data curation, methodology and writing the original draft with Mathilakath M. Vijayan; Helio Santos performed IHC and manuscript editing; Erin Faught designed and generated the founder populations, and edited the manuscript; Mathilakath M. Vijayan Conceptualization, funding acquisition, investigation and resource person, overall supervision of the project, writing the main text and editing. All authors have read and approved the final manuscript.

ACKNOWLEDGMENTS

This work was supported by a NSERC discovery grant (RGPIN-2019-06291) to Mathilakath M. Vijayan.

CONFLICT OF INTEREST STATEMENT

The authors declare no conflict of interest.

ORCID

Mathilakath M. Vijayan http://orcid.org/0000-0002-4300-1965

REFERENCES

Alsop, D., & Vijayan, M. M. (2008). Development of the corticosteroid stress axis and receptor expression in zebrafish. *American Journal of Physiology-Regulatory, Integrative and Comparative Physiology*, *294*(3), R711–R719. https://doi.org/10.1152/ajpregu.00671.2007

Arterbery, A. S., Fergus, D. J., Fogarty, E. A., Mayberry, J., Deitcher, D. L., Lee Kraus, W., & Bass, A. H. (2011). Evolution of ligand specificity in vertebrate corticosteroid receptors. *BMC Evolutionary Biology*, *11*(1), 14. https://doi.org/10.1186/1471-2148-11-14

Baker, M., Gaukrodger, N., Mayosi, B. M., Imrie, H., Farrall, M., Watkins, H., Connell, J. M. C., Avery, P. J., & Keavney, B. (2005). Association between common polymorphisms of the proopiomelanocortin gene and body fat distribution. *Diabetes*, *54*(8), 2492–2496. https://doi.org/10.2337/diabetes.54.8.2492

Baker, M. E., & Katsu, Y. (2017). 30 YEARS OF THE MINERALOCORTICOID RECEPTOR: Evolution of the mineralocorticoid receptor: sequence, structure and function. *Journal of Endocrinology*, *234*(1), T1–T16. https://doi.org/10.1530/JOE-16-0661

Balamurugan, K., Medishetti, R., Rao, P., K, R. V., Chatti, K., & Parsa, K. V. L. (2022). Protocol to evaluate hyperlipidemia in zebrafish larvae. *STAR Protocols*, *3*(4), 101819. https://doi.org/10.1016/j.xpro.2022.101819

Caprio, M., Fève, B., Claës, A., Viengchareun, S., Lombès, M., & Zennaro, M.-C. (2007). Pivotal role of the mineralocorticoid receptor in corticosteroid-induced adipogenesis. *The FASEB Journal*, *21*(9), 2185–2194. https://doi.org/10.1096/fj.06-7970com

Charmandari, E., Nicolaides, N. C., & Chrousos, G. P. (2014). Adrenal insufficiency. *The Lancet*, *383*(9935), 2152–2167. https://doi.org/10.1016/S0140-6736(13)61684-0

Charmandari, E., Tsigos, C., & Chrousos, G. (2005). Endocrinology of the stress response. *Annual Review of Physiology*, *67*(1), 259–284. https://doi.org/10.1146/annurev.physiol.67.040403.120816

Ehrhart-Bornstein, M., Hinson, J. P., Bornstein, S. R., Scherbaum, W. A., & Vinson, G. P. (1998). Intraadrenal interactions in the regulation of adrenocortical steroidogenesis. *Endocrine Reviews*, *19*(2), 101–143. https://doi.org/10.1210/edrv.19.2.0326

Elemans, L. M. H., Cervera, I. P., Riley, S. E., Wafer, R., Fong, R., Tandon, P., & Minchin, J. E. N. (2019). Quantitative analyses of adiposity dynamics in zebrafish. *Adipocyte*, *8*(1), 330–338. https://doi.org/10.1080/21623945.2019.1648175

Faillaci, F., Milosa, F., Critelli, R. M., Turola, E., Schepis, F., & Villa, E. (2018). Obese zebrafish: A small fish for a major human health condition. *Animal Models and Experimental Medicine*, *1*(4), 255–265. https://doi.org/10.1002/ame2.12042

Farooqi, I. S., Yeo, G. S. H., Keogh, J. M., Aminian, S., Jebb, S. A., Butler, G., Cheetham, T., & O'Rahilly, S. (2000). Dominant and recessive inheritance of morbid obesity associated with melanocortin 4 receptor deficiency. *Journal of Clinical Investigation*, *106*(2), 271–279. https://doi.org/10.1172/JCI9397

Faught, E., & Schaaf, M. J. M. (2023). The mineralocorticoid receptor plays a crucial role in macrophage development and function. *Endocrinology*, *164*(10), bqad127. https://doi.org/10.1210/endocr/bqad127

Faught, E., & Vijayan, M. M. (2018). The mineralocorticoid receptor is essential for stress axis regulation in zebrafish larvae. *Scientific Reports*, *8*(1), 18081. https://doi.org/10.1038/s41598-018-36681-w

Faught, E., & Vijayan, M. M. (2019). Postnatal triglyceride accumulation is regulated by mineralocorticoid receptor activation under basal and stress conditions. *The Journal of Physiology*, *597*(19), 4927–4941. https://doi.org/10.1113/JP278088

Faught, E., & Vijayan, M. M. (2020). Glucocorticoid and mineralocorticoid receptor activation modulates postnatal growth. *Journal of Endocrinology*, *244*(2), 261–271. https://doi.org/10.1530/JOE-19-0358

Faught, E., & Vijayan, M. M. (2022). Coordinated action of corticotropin-releasing hormone and cortisol shapes the acute stress-induced behavioural response in zebrafish. *Neuroendocrinology*, *112*(1), 74–87. https://doi.org/10.1159/000514778

Flynn, E. J., Trent, C. M., & Rawls, J. F. (2009). Ontogeny and nutritional control of adipogenesis in zebrafish (*Danio rerio*). *Journal of Lipid Research*, *50*(8), 1641–1652. https://doi.org/10.1194/jlr.M800590-JLR200

Gans, I. M., Grendler, J., Babich, R., Jayasundara, N., & Coffman, J. A. (2021). Glucocorticoid-responsive transcription factor Krüppel-Like factor 9 regulates fkbp5 and metabolism. *Frontiers in Cell and Developmental Biology*, *9*, 727037. https://doi.org/10.3389/fcell.2021.727037

Gonzalez Nunez, V. (2003). Identification of two proopiomelanocortin genes in zebrafish (*Danio rerio*). *Molecular Brain Research*, *120*(1), 1–8. https://doi.org/10.1016/j.molbrainres.2003.09.012

Gregoric, N., Groselj, U., Bratina, N., Debeljak, M., Zerjav Tansek, M., Suput Omladic, J., Kovac, J., Battelino, T., Kotnik, P., & Avbelj Stefanija, M. (2021). Two cases with an early presented proopiomelanocortin deficiency—A long-term follow-up and systematic literature review. *Frontiers in Endocrinology*, *12*, 1–13. https://doi.org/10.3389/fendo.2021.689387

Guo, C., Ricchiuti, V., Lian, B. Q., Yao, T. M., Coutinho, P., Romero, R., Li, J., Williams, G. H., & Adler, G. K. (2008). Mineralocorticoid receptor blockade reverses Obesity-Related changes in expression of adiponectin, peroxisome Proliferator-Activated Receptor-γ, and proinflammatory adipokines. *Circulation*, *117*(17), 2253–2261. https://doi.org/10.1161/CIRCULATIONAHA.107.748640

Harno, E., Gali Ramamoorthy, T., Coll, A. P., & White, A. (2018). POMC: The physiological power of hormone processing. *Physiological Reviews*, *98*(4), 2381–2430. https://doi.org/10.1152/physrev.00024.2017

Hulse, J. L., Habibi, J., Igbekele, A. E., Zhang, B., Li, J., Whaley-Connell, A., Sowers, J. R., & Jia, G. (2022). Mineralocorticoid receptors mediate diet-induced lipid infiltration of skeletal muscle and insulin resistance. *Endocrinology*, *163*(11), bqac145. https://doi.org/10.1210/endocr/bqac145

Kiilerich, P., Milla, S., Sturm, A., Valotaire, C., Chevolleau, S., Giton, F., Terrien, X., Fiet, J., Fostier, A., Debrauwer, L., & Prunet, P. (2011). Implication of the mineralocorticoid axis in rainbow trout osmoregulation during salinity acclimation. *Journal of Endocrinology*, *209*(2), 221–235. https://doi.org/10.1530/JOE-10-0371

De Kloet, E. R., Meijer, O. C., de Nicola, A. F., de Rijk, R. H., & Joëls, M. (2018). Importance of the brain corticosteroid receptor balance in metaplasticity, cognitive performance and neuro-inflammation. *Frontiers in Neuroendocrinology*, *49*, 124–145. https://doi.org/10.1016/j.yfrne.2018.02.003

De Kloet, E. R., Vreugdenhil, E., Oitzl, M. S., & Joëls, M. (1998). Brain corticosteroid receptor balance in health and disease. *Endocrine Reviews*, *19*(3), 269–301. https://doi.org/10.1210/edrv.19.3.0331

Klok, M. D., Alt, S. R., Irurzun Lafitte, A. J. M., Turner, J. D., Lakke, E. A. J. F., Huitinga, I., Muller, C. P., Zitman, F. G., Ronald de Kloet, E., & Derijk, R. H. (2011). Decreased expression of mineralocorticoid receptor mRNA and its splice variants in postmortem brain regions of patients with major depressive disorder. *Journal of Psychiatric Research*, *45*(7), 871–878. https://doi.org/10.1016/j.jpsychires.2010.12.002

Krude, H., Biebermann, H., Luck, W., Horn, R., Brabant, G., & Grüters, A. (1998). Severe early-onset obesity, adrenal insufficiency and red hair pigmentation caused by POMC mutations in humans. *Nature Genetics*, *19*(2), 155–157. https://doi.org/10.1038/509

Krude, H., & Grüters, A. (2000). Implications of proopiomelanocortin (POMC) mutations in humans: The POMC deficiency syndrome. *Trends in Endocrinology & Metabolism*, *11*(1), 15–22. https://doi.org/10.1016/s1043-2760(99)00213-1

Kühnen, P., Krude, H., & Biebermann, H. (2019). Melanocortin-4 receptor signalling: Importance for weight regulation and obesity treatment. *Trends in Molecular Medicine*, *25*(2), 136–148. https://doi.org/10.1016/j.molmed.2018.12.002

Kwan, W., Cortes, M., Frost, I., Esain, V., Theodore, L. N., Liu, S. Y., Budrow, N., Goessling, W., & North, T. E. (2016). The central nervous system regulates embryonic HSPC production via stress-responsive glucocorticoid receptor signaling. *Cell Stem Cell*, *19*(3), 370–382. https://doi.org/10.1016/j.stem.2016.06.004

Lefterova, M. I., Haakonsson, A. K., Lazar, M. A., & Mandrup, S. (2014). PPARγ and the global map of adipogenesis and beyond. *Trends in Endocrinology & Metabolism*, *25*(6), 293–302. https://doi.org/10.1016/j.tem.2014.04.001

Lightman, S. L., Birnie, M. T., & Conway-Campbell, B. L. (2020). Dynamics of ACTH and cortisol secretion and implications for disease. *Endocrine Reviews*, *41*(3), bnaa002. https://doi.org/10.1210/endrev/bnaa002

Linhart, K.-B., & Majzoub, J. A. (2008). Pomc knockout mice have secondary hyperaldosteronism despite an absence of adrenocorticotropin. *Endocrinology*, *149*(2), 681–686. https://doi.org/10.1210/en.2006-1136

McCormick, S. D., Regish, A., O'Dea, M. F., & Shrimpton, J. M. (2008). Are we missing a mineralocorticoid in teleost fish? Effects of cortisol, deoxycorticosterone and aldosterone on osmoregulation, gill Na+,K + -ATPase activity and isoform mRNA levels in Atlantic salmon. *General and Comparative Endocrinology*, *157*(1), 35–40. https://doi.org/10.1016/j.ygcen.2008.03.024

Medina, A., Seasholtz, A. F., Sharma, V., Burke, S., Bunney, W., Myers, R. M., Schatzberg, A., Akil, H., & Watson, S. J. (2013). Glucocorticoid and mineralocorticoid receptor expression in the human hippocampus in major depressive disorder. *Journal of Psychiatric Research*, *47*(3), 307–314. https://doi.org/10.1016/j.jpsychires.2012.11.002

Minchin, J., & Rawls, J. F. (2017). A classification system for zebrafish adipose tissues. *Disease Models & Mechanisms*, *10*(6), 797–809. https://doi.org/10.1242/dmm.025759

Mommsen, T. P., Vijayan, M. M., & Moon, T. W. (1999). Cortisol in teleosts: Dynamics, mechanisms of action, and metabolic regulation. *Reviews in Fish Biology and Fisheries*, *9*(3), 211–268. https://doi.org/10.1023/A:1008924418720

Nesan, D., & Vijayan, M. M. (2013). Role of glucocorticoid in developmental programming: Evidence from zebrafish. *General and Comparative Endocrinology*, *181*, 35–44. https://doi.org/10.1016/j.ygcen.2012.10.006

Nicolaides, N. C., Kyratzi, E., Lamprokostopoulou, A., Chrousos, G. P., & Charmandari, E. (2015). Stress, the stress system and the role of glucocorticoids. *Neuroimmunomodulation*, *22*(1–2), 6–19. https://doi.org/10.1159/000362736

Parasiliti-Caprino, M., Bollati, M., Merlo, F. D., Ghigo, E., Maccario, M., & Bo, S. (2022). Adipose tissue dysfunction in obesity: Role of mineralocorticoid receptor. *Nutrients*, *14*(22), 4735. https://doi.org/10.3390/nu14224735

Pippal, J. B., Cheung, C. M. I., Yao, Y.-Z., Brennan, F. E., & Fuller, P. J. (2011). Characterization of the zebrafish (*Danio rerio*) mineralocorticoid receptor. *Molecular and Cellular Endocrinology*, *332*(1), 58–66. https://doi.org/10.1016/j.mce.2010.09.014

Quinlivan, V. H., & Farber, S. A. (2017). Lipid uptake, metabolism, and transport in the larval zebrafish. *Frontiers in Endocrinology*, *8*, 1–11. https://doi.org/10.3389/fendo.2017.00319

Royan, M. R., Siddique, K., Csucs, G., Puchades, M. A., Nourizadeh-Lillabadi, R., Bjaalie, J. G., Henkel, C. V., Weltzien, F.-A., & Fontaine, R. (2021). 3D Atlas of the pituitary gland of the model fish medaka (*Oryzias latipes*). *Frontiers in Endocrinology*, *12*, 719843. https://doi.org/10.3389/fendo.2021.719843

Sakamoto, T., Yoshiki, M., Takahashi, H., Yoshida, M., Ogino, Y., Ikeuchi, T., Nakamachi, T., Konno, N., Matsuda, K., & Sakamoto, H. (2016). Principal function of mineralocorticoid signaling suggested by constitutive knockout of the mineralocorticoid receptor in medaka fish. *Scientific Reports*, *6*(1), 37991. https://doi.org/10.1038/srep37991

Santos, H. B., Thomé, R. G., Arantes, F. P., Sato, Y., Bazzoli, N., & Rizzo, E. (2008). Ovarian follicular atresia is mediated by heterophagy, autophagy, and apoptosis in *Prochilodus argenteus* and *leporinus taeniatus* (Teleostei: Characiformes). *Theriogenology*, *70*(9), 1449–1460. https://doi.org/10.1016/j.theriogenology.2008.06.091

Sathiyaa, R., & Vijayan, M. M. (2003). Autoregulation of glucocorticoid receptor by cortisol in rainbow trout hepatocytes. *American Journal of Physiology-Cell Physiology*, *284*(6), C1508–C1515. https://doi.org/10.1152/ajpcell.00448.2002

Shi, C., Lu, Y., Zhai, G., Huang, J., Shang, G., Lou, Q., Li, D., Jin, X., He, J., Du, Z., Gui, J., & Yin, Z. (2019). Hyperandrogenism in POMCa-deficient zebrafish enhances somatic growth without increasing adiposity. *Journal of Molecular Cell Biology*, *12*(4), 291–304. https://doi.org/10.1093/jmcb/mjz053

Soengas, J. L., Cerdá-Reverter, J. M., & Delgado, M. J. (2018). Central regulation of food intake in fish: An evolutionary perspective. *Journal of Molecular Endocrinology*, *60*(4), R171–R199. https://doi.org/10.1530/JME-17-0320

Sweeney, P., Gimenez, L. E., Hernandez, C. C., & Cone, R. D. (2023). Targeting the central melanocortin system for the treatment of metabolic disorders. *Nature Reviews Endocrinology*, *19*(9), 507–519. https://doi.org/10.1038/s41574-023-00855-y

Thompson, W. A., Rajeswari, J. J., Holloway, A. C., & Vijayan, M. M. (2024). Excess feeding increases adipogenesis but lowers leptin transcript abundance in zebrafish larvae. *Comparative biochemistry and physiology. Toxicology & pharmacology: CBP*, *276*, 109816. https://doi.org/10.1016/j.cbpc.2023.109816

To, T. T., Hahner, S., Nica, G., Rohr, K. B., Hammerschmidt, M., Winkler, C., & Allolio, B. (2007). Pituitary-Interrenal interaction in zebrafish interrenal organ development. *Molecular Endocrinology*, *21*(2), 472–485. https://doi.org/10.1210/me.2006-0216

Vijayan, M. M., Raptis, S., & Sathiyaa, R. (2003). Cortisol treatment affects glucocorticoid receptor and glucocorticoid-responsive genes in the liver of rainbow trout. *General and Comparative Endocrinology*, *132*(2), 256–263. https://doi.org/10.1016/S0016-6480(03)00092-3

Webster, M. J., Knable, M. B., O'Grady, J., Orthmann, J., & Weickert, C. S. (2002). Regional specificity of brain glucocorticoid receptor mRNA alterations in subjects with schizophrenia and mood disorders. *Molecular Psychiatry*, *7*(9), 985–994. https://doi.org/10.1038/sj.mp.4001139

Weinstock, P. H., Levak-Frank, S., Hudgins, L. C., Radner, H., Friedman, J. M., Zechner, R., & Breslow, J. L. (1997). Lipoprotein lipase controls fatty acid entry into adipose tissue, but fat mass is preserved by endogenous synthesis in mice deficient in adipose tissue lipoprotein lipase. *Proceedings of the National Academy of Sciences*, *94*(19), 10261–10266. https://doi.org/10.1073/pnas.94.19.10261

Wood, A. W., Duan, C., & Bern, H. A. (2005). Insulin-Like Growth Factor Signaling in Fish, *In* International Review of Cytology (Vol. 243, p. 215–285). Academic Press. https://doi.org/10.1016/S0074-7696(05)43004-1

Yang, Z., Wong, J., Wang, L., Sun, F., & Yue, G. H. (2023). Pomc knockout increases growth in zebrafish. *Aquaculture*, *574*, 739707. https://doi.org/10.1016/j.aquaculture.2023.739707

Zang, L., Maddison, L. A., & Chen, W. (2018). Zebrafish as a model for obesity and diabetes. *Frontiers in Cell and Developmental Biology*, *6*, 256–564. https://doi.org/10.3389/fcell.2018.00091

Zhang, C., Forlano, P. M., & Cone, R. D. (2012). AgRP and POMC neurons are hypophysiotropic and coordinately regulate multiple endocrine axes in a larval teleost. *Cell Metabolism*, *15*(2), 256–264. https://doi.org/10.1016/j.cmet.2011.12.014

SUPPORTING INFORMATION

Additional supporting information can be found online in the Supporting Information section at the end of this article.

How to cite this article: Rajeswari, J. J., Faught, E., Santos, H., & Vijayan, M. M. (2024). Mineralocorticoid receptor activates postnatal adiposity in zebrafish lacking proopiomelanocortin. *Journal of Cellular Physiology*, *239*, e31428. https://doi.org/10.1002/jcp.31428